JACC: CARDIOVASCULAR IMAGING
VOL. 10, NO. 4, 2017

ISSN 1936-878X/$36.00
PUBLISHED BY ELSEVIER

iMAIL

LETTERS TO THE EDITOR

[^{18}F]-NaF PET/CT Identifies Active Calcification in Carotid Plaque

Although macroscopic calcium deposits in atherosclerotic plaques impart stability, microcalcific deposits can amplify mechanical stress in the fibrous cap by 600 kPa (1). Blood flow, stress, and tension between calcified and noncalcified tissue can increase the risk of plaque rupture. It is postulated that [^{18}F]-sodium fluoride (^{18}F-NaF) imaged with positron emission tomography (PET) replaces the hydroxyl groups of hydroxyapatite, expressed in regions with active microcalcification (2). Validation of ^{18}F-NaF as an imaging-derived biomarker of hydroxyapatite in atherosclerotic plaque is required.

Eleven patients (69 ± 5 years old, 3 women) with high-risk cerebrovascular disease who were scheduled for endarterectomy were recruited. ^{18}F-NaF PET/computed tomography (CT) imaging of the carotid vasculature was acquired within 2 weeks before surgery. Institutional ethics committee review approval was obtained (OHSN-REB 20120224-01H). Patients provided informed consent. Sixty min after ^{18}F-NaF injection (3 MBq/kg), PET/CT imaging was performed, followed by CT angiography (Discovery 690 PET-VCT, GE Medical Systems, Milwaukee, Wisconsin). Radiation effective dose was 9 mSv. One patient could not complete imaging.

^{18}F-NaF PET/CT images were coregistered with a HybridViewer (Hermes Medical Solutions, Greenville, North Carolina). ^{18}F-NaF uptake (Bq/cc) was normalized to injected activity and body weight (standardized uptake value [SUV]). Plaque SUV was normalized to the mean SUV of blood in the internal jugular vein (tissue-to-blood ratio [TBR]). Bilateral carotid ^{18}F-NaF uptake was quantified by: 1) a vessel-based approach to define maximum ^{18}F-NaF uptake for each PET slice spanning 2 cm above and below the bifurcation (TBR_{vessel}, SUV_{vessel}); and 2) a foci-based approach for determining the maximum ^{18}F-NaF activity for each plaque (TBR_{max}, SUV_{max}).

En bloc excised plaque was sectioned and stained with Goldner's trichrome [hydroxyapatite (3)] and Alizarin Red S (extent of calcification). The extent of staining was quantified with color-encoded digitized slides (Aperio Technologies, Vista, California). The carotid bifurcation was identified on digitized 3-dimensional histology images and located on CTA and PET to coregister with histology.

Bilateral carotid plaques were classified as either associated with patient symptoms (transient ischemic attacks or stroke; 9 plaques) or not (11 plaques). Plaque associated with symptoms had evidence for greater ^{18}F-NaF uptake than plaque not associated with symptoms (TBR_{max}: 3.75 ± 1.10 vs. 2.79 ± 0.60; $p = 0.04$; SUV_{max}: 3.00 ± 0.90 vs. 2.40 ± 0.80; $p = 0.125$). ^{18}F-NaF uptake was related to Goldner's trichrome expression (TBR_{vessel}: $r = 0.45$; $p < 0.001$; SUV_{vessel}: $r = 0.43$; $p < 0.001$) but not Alizarin Red S (TBR_{vessel}: $r = 0.12$; $p = 0.36$; SUV_{vessel}: $r = -0.05$; $p = 0.73$) (**Figure 1**). To account for intraplaque clustering of data, a fixed-effects model for combining correlations with weights inversely related to within-patient variation was used. This compared the independent and individual correlation between ^{18}F-NaF uptake and staining for each plaque. Findings confirmed the ^{18}F-NaF TBR_{vessel} and Goldner's trichrome relationship ($r = 0.37$; $p = 0.006$) (**Figure 1**).

Elevated ^{18}F-NaF uptake observed in plaque associated with patient symptoms might reflect active microcalcific processes. Microcalcification could increase the risk of mechanical failure, contributing to plaque instability (1). It is proposed that sodium fluoride replaces the hydroxyl groups of hydroxyapatite (2). Supporting this hypothesis, the present study validates the relationship between in vivo ^{18}F-NaF uptake and ex vivo hydroxyapatite expression within carotid plaque. ^{18}F-NaF uptake was related to active microcalcification (hydroxyapatite expression) rather than the overall extent of calcification (Alizarin Red S), which suggests that ^{18}F-NaF selectively targets the regions of active calcification.

Study limitations include the recognized challenges with coregistration of PET/CT images against histology; the absence of alkaline phosphatase validation, although this has been reported by others (4); and the fact that this was a small proof-of-concept study.

Calcium has been considered to be a static, aplastic amorphous material. This is in part because of the lack of technology available to assess the dynamic nature of calcification, which renders the potential impact and prognostic relevance of active calcification virtually unexplored. Our findings demonstrate that ^{18}F-NaF imaging can noninvasively identify active calcification.

FIGURE 1 ^{18}F-NaF is a Surrogate Marker of Active Calcification in Carotid Plaque

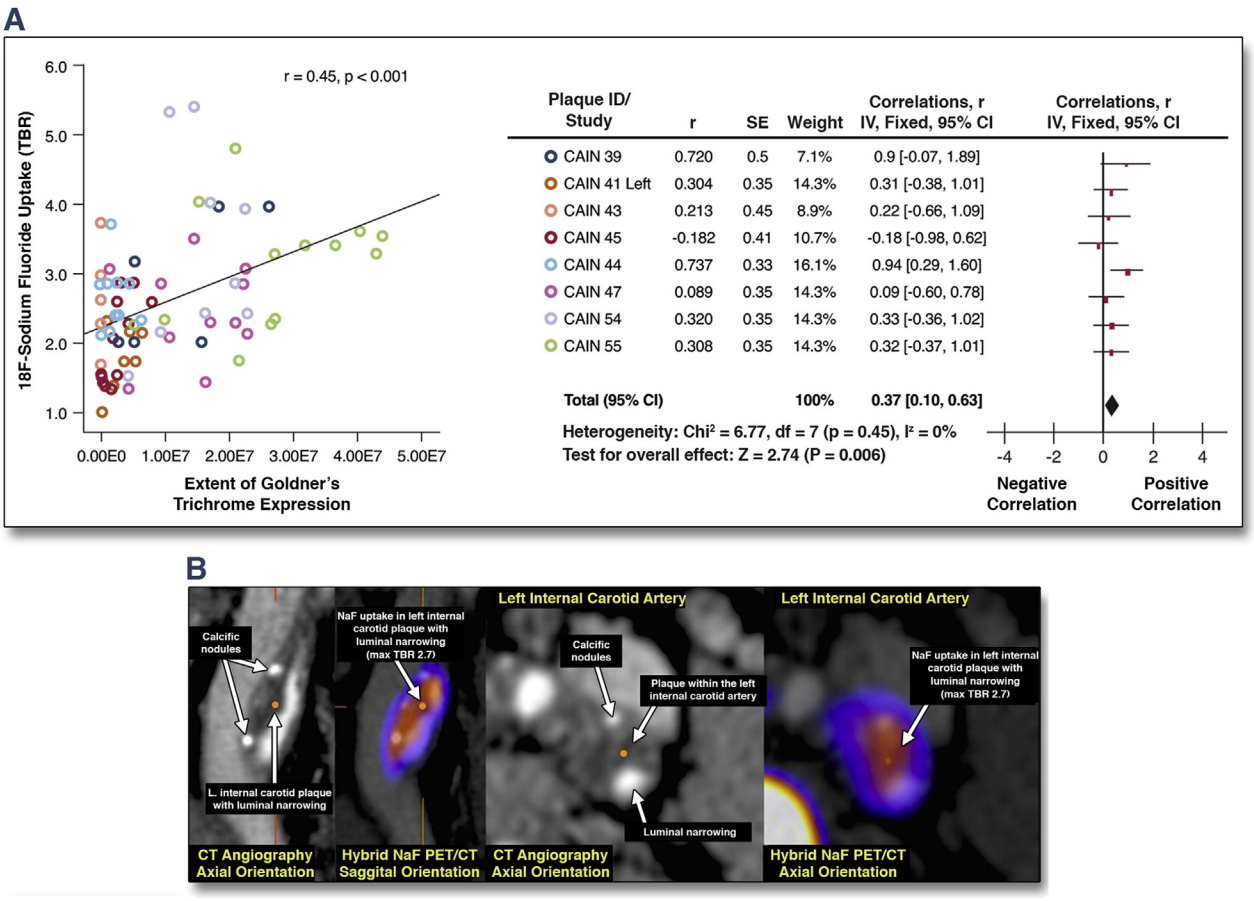

(A) [^{18}F]-sodium fluoride (^{18}F-NaF) uptake correlation with hydroxyapatite expression; intraplaque clustering is noted **(left)**; fixed-effects model for individual lesion correlations (r = 0.37, p = 0.006) **(right)**. **(B)** ^{18}F-NaF uptake encompasses a greater region than calcific nodules within plaque **(left)**. CAIN = Canadian Atherosclerosis Imaging Network; CI = confidence interval; CT = computed tomography; df = degrees of freedom; IV = inverse variance; L = left; PET = positron emission tomography; TBR = tissue-to-blood ratio.

Myra S. Cocker, PhD
J. David Spence, MD
Robert Hammond, MD
George Wells, PhD
Robert A. deKemp, PhD
Cheemun Lum, MD
Adebayo Adeeko, PgDip
Martin J. Yaffe, PhD
Eugene Leung, MD
Andrew Hill, MD
Sudhir Nagpal, MD
Grant Stotts, MD
Murad Alturkustani, MD
Laurel Hammond
Jean DaSilva, PhD
Tayebah Hadizad, PhD
Jean-Claude Tardif, MD

Rob S.B. Beanlands, MD*
for the Canadian Atherosclerosis Imaging Network (CAIN)
*Division of Cardiology
National Cardiac PET Centre
University of Ottawa Heart Institute
40 Ruskin Street
Ottawa, Ontario, K1Y 4W7
Canada
E-mail: rbeanlands@ottawaheart.ca

http://dx.doi.org/10.1016/j.jcmg.2016.03.005

Please note: This work was supported by the Canadian Institutes of Health Research grant #CRI-88057. Dr. Cocker was a Research Fellow of the Heart and Stroke Foundation (HSF) of Canada and is currently the Ottawa Heart Institute Ernest & Margaret Ford Fellow. Dr. Beanlands is a Career Investigator supported by the HSF, Tier 1 Ottawa Research Chair and Vered Chair in Cardiology; and has been a consultant for and received grant funds from GE Healthcare. All other authors have reported that they have no relationships relevant to the contents of this paper to disclose. The findings of this study have been presented in part at the American Heart

Association Scientific Sessions 2014 and the Canadian Cardiovascular Congress 2014.

REFERENCES

1. Vengrenyuk Y, Carlier S, Xanthos S, et al. A hypothesis for vulnerable plaque rupture due to stress-induced debonding around cellular microcalcifications in thin fibrous caps. Proc Natl Acad Sci U S A 2006;103:14678–83.

2. Blau M, Ganatra R, Bender MA. 18 F-fluoride for bone imaging. Semin Nucl Med 1972;2:31–7.

3. Fitzpatrick LA, Severson A, Edwards WD, Ingram RT. Diffuse calcification in human coronary arteries. Association of osteopontin with atherosclerosis. J Clin Invest 1994;94:1597–604.

4. Irkle A, Vesey AT, Lewis DY, et al. Identifying active vascular microcalcification by (18)F-sodium fluoride positron emission tomography. Nat Commun 2015;6:7495.

Percutaneous Bicuspidization of the Tricuspid Valve

A 75-year-old woman who was known to have had previous aortic and mitral valve replacement with mechanical prostheses, permanent atrial fibrillation, type 2 diabetes mellitus, and hypothyroidism presented with right-sided heart decompensation (severe edema of the lower extremities, pleural effusion, hepatomegaly, and stage IV chronic kidney disease). Echocardiography showed massive functional tricuspid regurgitation due to severe tricuspid annulus dilatation (diameter 49 × 37 mm) and complete absence of leaflet coaptation (**Figure 1A**); a severely dilated right ventricle (end-diastolic diameter 43 mm) with moderate dysfunction (TDI S′ 10 cm/s); systolic pulmonary arterial pressure 40 mm Hg; noncollapsible inferior vena cava with estimated right atrial pressure of 20 mm Hg; normal left ventricular function; normal gradients across mitral and aortic prosthetic valves; and mitral paravalvular leak with moderate mitral regurgitation.

Intravenous high-dose diuretic therapy was able to reduce systemic congestion and to improve kidney function: however, the patient was dependent on intravenous diuretic agents, and conversion to oral therapy was not achievable. The patient was not suitable for surgical treatment of tricuspid regurgitation because of high operative risk (logistic EuroSCORE [European System for Cardiac Operative Risk Evaluation] 24%).

A compassionate percutaneous treatment of the tricuspid valve was chosen: the Trialign system (Mitralign Inc., Tewksbury, Massachusetts) was used to plicate the tricuspid annulus, as described previously by Schofer et al (1). This procedure, which resembles the surgical Kay procedure with bicuspidization of the tricuspid valve via plication of the posterior leaflet, was performed under general anesthesia, with fluoroscopic and 3-dimensional echocardiographic guidance. The procedure was performed by a right transjugular approach with 2 14-F sheaths and steerable guiding catheters. An articulating 8-F wire delivery catheter was introduced in a retrograde fashion across the tricuspid valve through one of the 14-F guiding catheters. The catheter was articulated under the annulus to the posteroseptal commissure; an insulated radiofrequency wire was then advanced across the annulus into the right atrium at a distance of 2 to 5 mm from the base of the leaflet. This wire was snared via the second 14-F sheath, externalized, and used to advance the pledget catheter anterogradely across the annulus. Half the pledget was delivered and cinched in the subannular region of the ventricle, whereas the remaining pledget was extruded and cinched on the atrial surface of the tricuspid annulus. Another pledget was delivered in a similar manner on the anteroposterior commissure at a distance of 2.4 to 2.8 cm from the first pledget. At the end, the 2 pledgets were placed at the base of the posterior leaflet, near the anteroposterior and posteroseptal commissure. The 2 pledgeted sutures were pulled together with a plication lock catheter, and the sutures were cut, which resulted in plication of the tricuspid annulus (**Figures 1B and 1C**), thus effectively making the tricuspid valve bicuspid (**Figure 1D**); this translated to a significant reduction in annular dimensions (31 × 23 mm) and valve planimetric area (14.9 to 5.6 cm^2), increased coaptation of the leaflets, and reduction of final tricuspid regurgitation to moderate-severe with a large reduction in effective regurgitant orifice area (4.7 to 1.1 cm^2) (**Figures 1E and 1F**). No changes were documented in estimated systolic pulmonary arterial pressure (38 mm Hg) and right atrial pressure (20 mm Hg). A significant improvement in clinical status was achieved; intravenous diuretic discontinuation was possible, and the patient was discharged with high-dose oral diuretic therapy. This case highlights that the Trialign provides a novel solution for percutaneous tricuspid valve repair by replicating surgical bicuspidization of the tricuspid valve. Patient selection and defining the correct outcome measures will be an essential part of investigating this innovative therapy in this complex patient cohort.